CoRoT: Description of the Mission and Early Results

Annie Baglin[1], Michel Auvergne[1], Pierre Barge[2], Magali Deleuil[2], Eric Michel [1] and The CoRoT Exoplanet Science Team

[1]LESIA, Observatoire de Paris, 92315 Meudon, France
email: `annie.baglin@obspm.fr`
[2]LAM, Marseille, France
email: `pierre.barge@oamp.fr`

Abstract. The CoRoT Mission and its performances in flight are summarised. After more than 500 days in orbit, the early results in the exoplanet finding programme are highlighted. The first 5 planets discovered are compared to the previous population of exoplanets.

1. Overall description of the mission

The CoRoT mission performs ultra-high-precision photometry from space. The major specification is a maximum noise level of 0.6 ppm in 5 days for a 5.7 magnitude star. A very long duration of the observations, from 25 to 150 days, with a duty cycle larger than 90 % is also required; see for instance Baglin *et al.* (2002).

It has two major scientific programmes: stellar seismology around the HR diagram and search for small extrasolar planets. It will also perform important additional science on a variety of astrophysical topics, as described in Weiss *et al.* (2004). It is an intermediate-size mission, which had to be installed on a PROTEUS platform (Landiech and Douillet 2004). This bus has been designed for low-Earth-orbit Small Missions. It limits the total weight of the satellite to 600 kg, the available power onboard to 1 kW and the scientific telemetry rate to 1.5 Gbits per day.

CoRoT has been funded mostly by France. Six european partners and Brazil contributed to the payload and the ground segment. The payload has been built under CNES as prime contractor, with a large contribution of 3 french laboratories. It has been launched by a Soyuz II-1b rocket, as its maiden flight, from the Baïkonour cosmodrome on December 27th 2006 at 14:23:38 UT.

The orbit is polar at an altitude of 897 km and the launch was perfect, needing no correction of the trajectory. At the time of the IAU 253 Symposium it had spent 510 days in orbit.

The observations are done in the continuous viewing zones : two circles of approximately 10 degrees radius, centered at the intersection of the celestial equator and the galactic plane, in opposite directions.

The instrument is described in details in the CoRot Book (CoRoT 2006). Its in-flight performances are evaluated in Auvergne *et al.* (2008), where it is shown that the quality of the instrument associated to the data correction chain reaches the objectives of the scientific programme.

Figure 1. General view of the CoRoT instrument during its integration phase, at CNES, Toulouse, France. Its total height is 3.4 m.

2. Stellar seismology and variability

The seismology programme is very successful, as presented for instance by Michel *et al.* (2008a).

The solar like oscillations are detected for all the solar like stars observed so far, and it is possible to distinguish the p-mode spectrum from the granulation contribution and to measure their global properties (Michel *et al.* 2008b). In the bright solar-like oscillator observed during the first run of 60 days, more than 40 independant modes have been detected and their frequency measured with an accuracy of $\sim 1\ \mu Hz$.

Pulsations are detected and interpreted in many red giants and in almost all Be stars. Large-amplitude pulsators have a very rich spectrum of modes with lower amplitudes than the ones detected from the ground. They are still difficult to decipher.

At the photometric accuracy reached by CoRoT, almost 50 % of stars are variables (Fig. 2). The very large sample of objects already observed (more than 20 000) in the exoplanet field (Fig. 3) covers all types of already known variability but also the detection of microvariabilities like those due to spotted rotating stars and to surface phenomena like granulation and activity. An automatic classification is underway (Debosscher *et al.* 2007).
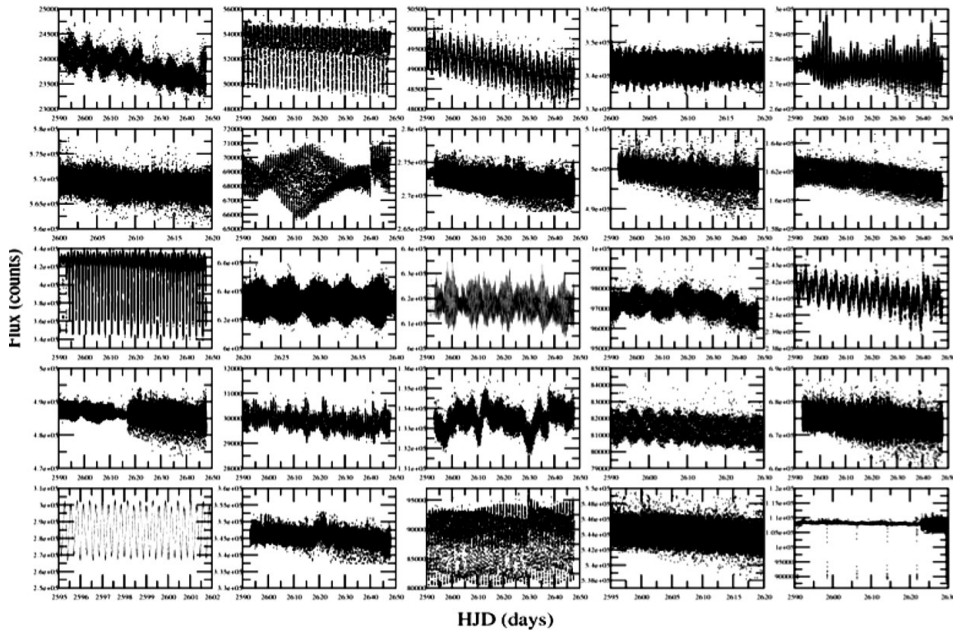
Figure 2. A selection of variables as seen by CoRoT during the inital run IRa01, over 60 days.

3. The exoplanet programme

3.1. *The exoplanet field and the data collection*

As seen on Fig. 3, the focal plane is shared by the two programmes, which work simultaneously on adjacent regions of the sky.
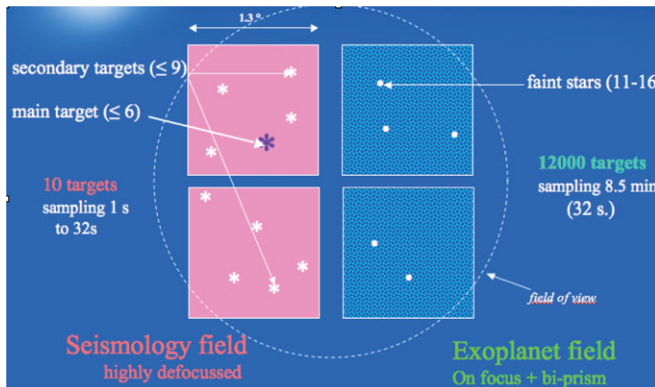

Figure 3. The focal plane and its 4 detectors.

Data for the exoplanet programme are gathered on 2 EEV CCDs. They are frame transfer, thinned back illuminated, with 2048x2048 pixels. The pixel size is 13.5μ or 2.32 arc sec.

A dispersive device of very low resolution (~ 4) allows to separate the "blue", "green" and "red" part of the stellar image, at least for the bright targets.
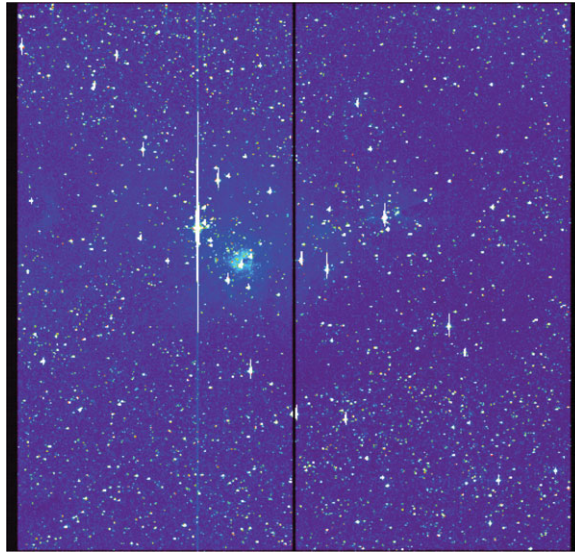
Figure 4. The exoplanet field of the run SRa01, centered on the young cluster NGC 2264, obtained by adding 160 exposures of 32 s each . Elongated bright structures are due to saturation from the bright stars of the field. The cluster is located in the light blue region. In this image almost 6000 targets have been observed.

A full image of one the detectors for the SRa01 run centered on the cluster NGC 2264, is shown on Fig. 4.

Aperture photometry is then performed, using a set of 256 templates, which are ajusted directly on the CoRoT image, taking into account its local properties. An example of this process is given in Fig. 5.

On each detector up to 6000 targets can be observed at the same time. They are selected individually and/or statistically. Priority is given to the brighter F, G , K and M dwarfs, with low contamination by neighbors (Fig. 6).

3.2. *Unexpected sources of noise*

The low-earth orbit was expected to be the major source of perturbators to the photo-metric signal. Pre-launch studies had shown that they can be handled and corrected to reach the scientific specifications, as described in the CoRoT Book (CoRoT 2006).

Some perturbations not foreseen before had to be understood and taken into account in the correction pipe-line. The two most important ones are described below.

The detectors are hit by heavy charged particles during the South Atlantic Anomaly crossing. With transient events, protons impact also produce permanent hot pixels due mainly to atomic displacements in the silicon lattice. The intensity of a bright pixel is not stable in time. On short time scales (few minutes to few hours) phase rearrangement induces abrupt or exponential decrease of the intensity. A long term annealing often follows, and a bright pixel can disappear after several days to a few years, as seen on Fig. 7 (Pinheiro *et al.* 2008).

It is easy to get rid of the photometric perturbation due to a hit in a background window, but it is more difficult when the hot pixel is on the stellar image itself. It is estimated that their number will reach 5% of the total number of pixels at the end of the mission (Fig. 8).
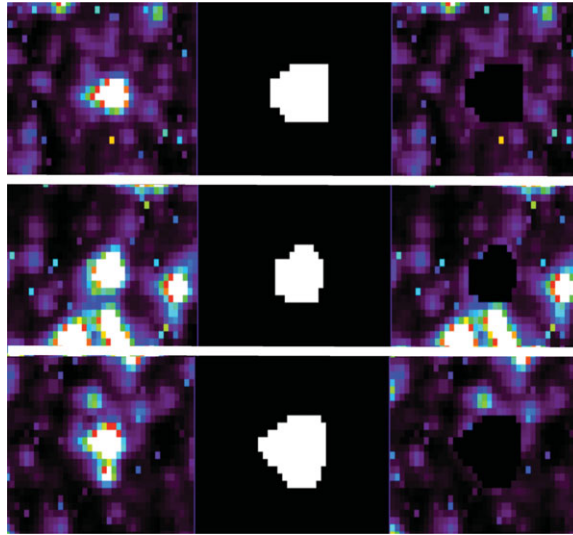
Figure 5. The aperture photometry and the template adjustment. On each row, the left image is the sky image around a proposed target, as seen by CoRoT; the middle one is the mask adjusted to the image (in white), and the right one is the difference, showing the efficiency of the template. The first row corresponds to an isolated target, for which the mask matches nicely the PSF; on the second row, the target is contaminated, and the mask is adjusted to avoid the contaminants, as efficiently as possible; on the third row the star and its contaminant cannot be separated and are included in a broader single mask.
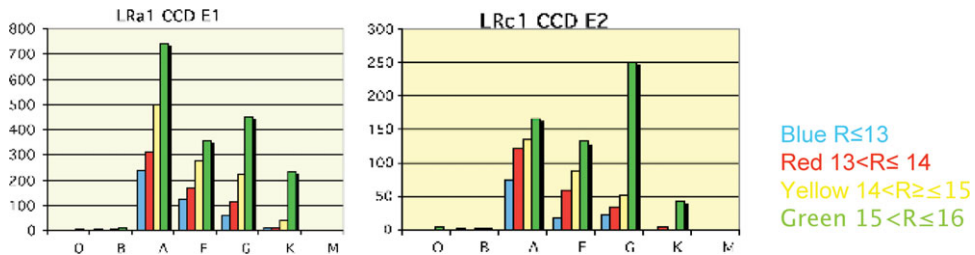

Figure 6. Example of the population of stars on the exoplanet CCDs for two different pointings.

The ingress/egress from the Earth eclipses induces attitude perturbations of the satellite, which influence the photometric measurement. The crossing of the eclipsing zone of the satellite induces power perturbations and vibrations of the solar panels during some tens of seconds. It produces depointings which can be as large as a few pixels. Such depointings were not foreseen, and their photometric perturbations remain difficult to correct (Fig. 9).

In addition, there are still some rare and yet unexplained events.

3.3. *Photometric performances in the exoplanet field*

The present performances as a function of the R magnitude in white light are given in Fig. 10.

They have been measured by selecting the "less" variable stars per magnitude interval, then building an average light curve using a SVD, and compute the mean value of the power spectrum between 1 day and 2 hours. At $R = 12.5$, $\sigma = 7 \cdot 10^{-4}$ over 512 s,
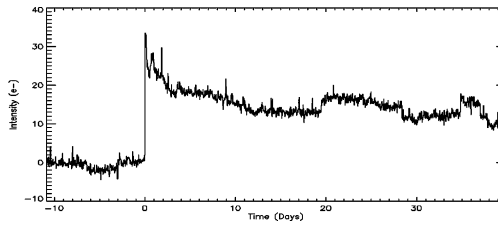
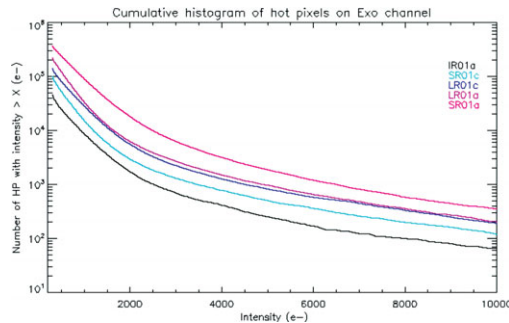**Figure 7.** The behavior of a hot pixel as a function of time.

Figure 8. Evolution of the number of pixels with time. Measurements have been made at the beginning of the 5 first runs. The abscissa axis is the energy of the hot pixel.
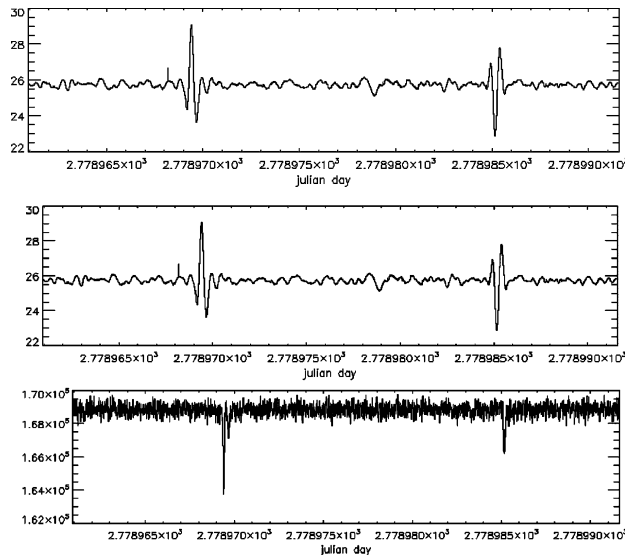

Figure 9. Depointings measured in the direction of the line of the CCD and associated photometric perturbations during an ingress, then an egress of the eclipsing zone.

which is very close to the scientific specification. Assuming a transit duration of 3 hours it corresponds to a detection level of $1.5 \cdot 10^{-4}$.
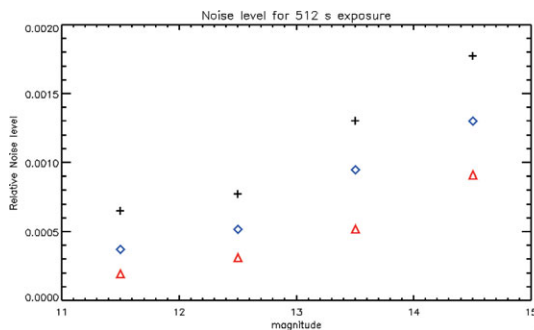
Figure 10. Photometric performances of the exoplanet channel. Red triangles correspond to the white noise level (theoretical $1/N^{1/2}$ photon noise + readout noise + background noise), blue diamonds correspond to the rms measured on the white light curve during a period without eclipses (small jitter perturbations) and black crosses the rms measured on the white light curve during the total duration of the run.

4. The present CoRoT family of exoplanets

4.1. *The detection of candidates*

To detect planet candidates, there are 8 groups of transit sniffers working independently (See Barge *et al.* in this volume). Their methods have been tested before launch through Hare and Hounds exercises on simulated data (Moutou *et al.* 2007).

The detection process is using two types of data:
- the "alarm data" produced rapidly every week during the observations, to detect possible transits very rapidly, to trigger oversampling of a suspected transiting target at 32s on board as soon as possible.
- the fully reduced data (called N2).

For the three runs already achieved, the detection have been made only on the alarm data yet. Over the 11 000 targets on each run, more than 200 candidates have been detected.

Presently, the smallest transit detected has a depth of a few 10^{-4}, corresponding to a planetary radius of $\sim 2\ R_{earth}$ (if it is a planet !). The nature of the transiting object is under study from the ground (Fig. 11).

4.2. *The five first confirmed planets*

Among those several hundred candidates, 5 planets are presently firmly confirmed, thanks to follow-up observations using on/off photometry and then spectroscopy from the ground (see Bouchy *et al.* in this volume). The main characteristics of the planets and their parent stars are given in Table 1.

Among the 5 confirmed planets, systems with quite specific properties are discovered:

CoRot-exo-1b , at 1 M_{Jup} has a quite low density (Barge *et al.* 2008),

CoRot-exo-2b is a massive Hot Jupiter around a very active star. Note that 81 successive transits have been observed (Alonso *et al.* 2008, Bouchy *et al.* 2008),

CoRot-exo-3b is a transition object between planets and brown dwarfs (Deleuil *et al.* 2008),

CoRot-exo-4b has the longest period detected, and seems to be synchronised to the rotation period of the star (Aigrain *et al.* 2008, Moutou *et al.* 2008),

CoRot-exo-5b is a standard Hot Jupiter with 4-day period, but the orbit is probably highly excentric (Rauer *et al.* 2008).
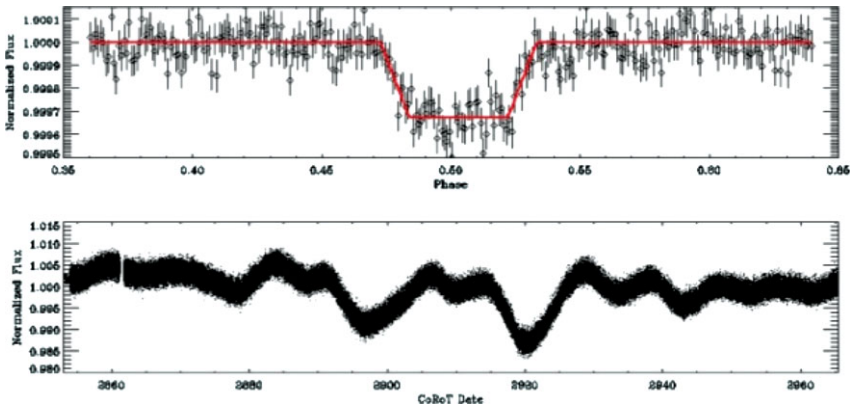
Figure 11. Light curve of a target containing a planet candidate during the whole observation of 140 days (bottom), and phase folding of the region of the detected transit. Note the U shape, characteristic of a planetary transit.

Table 1. Characteristics of the planets and the parent stars discovered and confirmed by CoRoT at the date of the symposium.

Planet[0]	R[1] (star)	N transits	Period	Duration	Radius[2]	Mass[2]	Teff[3] (star)	Mass[4] (star)
1	13.6	36	1.509	2.4	1.49 ± 0.1	1.03	5950	0.95 ± 0.15
2	12.57	81	1.743	2.3	1.465 ± 0.05	3.31	5625	0.97 ± 0.1
3	13.3	34	4.26	3.8	0.97 ± 0.1	21.6	6630	1.37 ± 0.1
4	13.7	6	9.202	3.8	1.18 ± 0.3	0.72	6190	1.19 ± 0.1
5	14	27	4.03	3.2	1.16 ± 0.036	1.01	6000	1.2 ± 0.1

Notes:
[0] The CoRoT identifier of the discovered planet is CoRoT-exo-nb, and the parent star is named CoRoT-exo-n.
[1] R magnitude of the parent star from Exodat (Deleuil *et al.* 2008).
[2] Radius and mass of the planet in Jupiter units.
[3] Effective temperature of the parent star from spectroscopic detailed analysis.
[4] Evolutionary mass of the parent star from position in the $M/R^{1/3}, T_{eff}$ plane.

4.3. *Stellar parameters, a critical issue*

As both mass and radius of the planet are measured relative to the host star ones, the determination of the radius and mass of the host star is a critical issue. It proceeds by two succesive steps: a detailed spectral analysis and then a stellar evolution modeling.
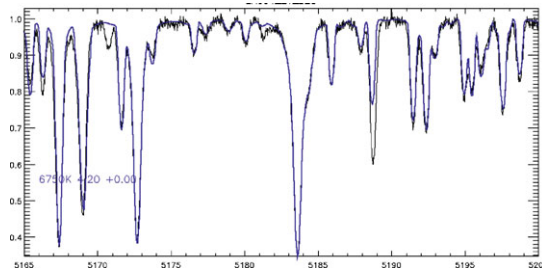

Figure 12. Model atmosphere fitting in the range 5150-5200 Å, for CoRoT-exo-2.

For the faint stars of the CoRoT programme, detailed spectral analysis cannot reach a better precision than 200K in T_{eff} and 0.2 *dex* in Fe/H (Fig. 12), even using very large telescopes; *log g* is generally badly defined. Also deviations of individual abundances from a typical solar mixture are frequent.

Stellar evolution modeling can be adapted to the case of transiting planets where the timing of the transit gives a very precise observable $M^{1/3} R^{-1}$. So evolutionnary tracks can be drawn in the $logT_{eff}$, $M^{1/3} R^{-1}$ plane, (Fig. 13). Typical uncertainties are 10 to 20% in mass, 10 to 20% in radius. A large part is due to the uncertainty on the chemical composition. The age determination from the model comparison is very uncertain, especially for stars close to the main sequence, where the fundamental parameters change very slowly. This quantity needs to be evaluated using other indicators such as activity, but they are also subject to large uncertainties.
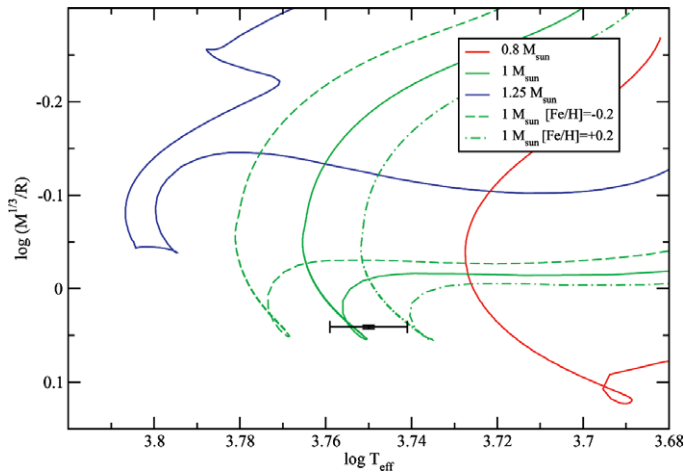

Figure 13. Modeling CoRot hosting star CoRoT-exo-2 in the $logT_{eff}$, $M^{1/3} R^{-1}$ plane.

4.4. *Contribution to the Mass/Radius relation*

The position of the CoRoT planets in the Mass Radius diagram are shown in Fig. 14. Four of them occupy a quite marginal position. Though it is too early to draw firm conclusions, it gives the impression that such a systematic survey, only magnitude limited, allows to reach a large coverage of the parameters of the star-planet system, leading to the discovery of original objects.

5. And then...

The mission is working very well and could be continued for several years after the 3 year nominal duration. Both the onboard and ground segments have reached their mature status. Data are being produced and distributed faster than expected.

The period/depth diagram (Figure 3 in Barge *et al.*, this volume) plotting all the detected transits during the first two runs is filled with events in all the domain specified by the scientific programme. This demonstrates that the instrumental performances are very satisfactory, and that CoRoT is able to detect transiting telluric planets if they exist.

The ground based follow-up associated programme is a long and time consuming process. It needs large and generally oversubscribed instruments. So, one has to get used
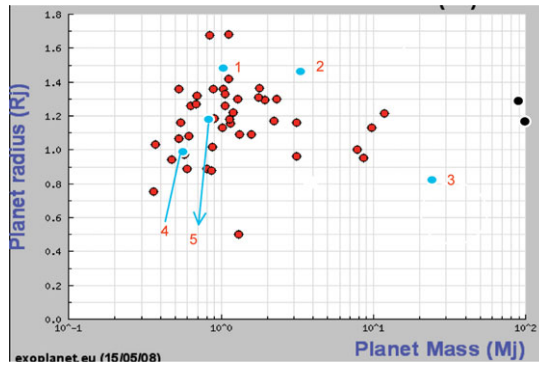
Figure 14. The CoRoT planets in the Mass-Radius diagram.

to the fact that confirming a planet, especially if it is small, is a long story after the detection of the photometric event.

In addition to the "Core" programme of seismology and planet detection, the observation of stellar variability at the 10^{-4} level, continuously over up to 150 days, is a gold mine for stellar physicists.

CoRoT, though a small mission, is evidently a wonderful tool, but still difficult to master. It opens the road to the other photometric missions KEPLER and then PLATO. Let us hope that the experience gained in this pionner mission will be helpful to optimise the future ones.

6. Acknowledgments

References

Aigrain, S., Collier-Cameron, A., Ollivier, M., Pont, F., Jorda, L. *et al.* 2008, *Astron. & Astrophys. Letter*, in press.

Alonso, R., R., Auvergne, M., Baglin, A., Ollivier, M., Moutou, C. *et al.* 2008, *Astron. & Astrophys.*, 418 L21.

Auvergne, M., Boisnard, L., Lam-Trong. T *et al.*;, 2008 *Astron. & Astrophys.*, submitted.

Baglin, A., Auvergne, M., Barge, P., *et al.*: 2002, *ESA-SP*, 481, 17.

Barge, P., Baglin, A., Auvergne, M., Rauer, H., Léger, A. *et al.* 2008, *Astron. & Astrophys.*, 418, L17.

Bouchy, F., Queloz, D., Deleuil, M., Loeillet, B., Hatzes, A. P., Aigrain, S., Alonso, R., Auvergne, M., Baglin, A., Barge, P., *et al.*: 2008 *Astron. & Astrophys.* 482, L25.

The CoRoT Mission: pre-launch status: 2006 ESA-SP 1306, eds M. Fridlund, A. Baglin, L. Conroy & J. Lochard.

Debosscher, J., Sarro, L. M., Aerts, C., Cuypers, J., Vandenbussche, B. *et al.*: 2007 *Astron. & Astrophys.* 475, 1159.

Deleuil, M., Deeg, H., Alonso, R., Bouchy, F., Rouan, D. *et al.* 2008, *Astron. & Astrophys.*, accepted.

Landiech, P., Douillet F.:2004, *Small Satellite System and Services, symposium ESA SP-571*, B. Warmbein edt., p. 1.1. J. Geophys. Res.

Michel, E., Baglin, A., Weiss, W. *et al.*: 2008 *Wroclaw Helas workshop, eds. W. Dziembovsky, M. Breger and M. Thompson, CoAst. submitted.*

Michel, E., Baglin, A., Auvergne, M., Catala, C., Samadi, R., Baudin, F., Appourchaux, T., Barban, C. Weiss, W. *et al.* : 2008 *Science* , in press.

Moutou, C., Pont, F., Barge, P., Aigrain, S.,Auvergne, M., Blouin, D., Cautain, R., Erikson, A. R., Guis, V., Guterman, P., Irwin, M., Lanza, A. F., Queloz, D., Rauer, H., Voss, H., & Zucker, S.: 2007 *Astron. & Astrophys.* 437, 355.

Moutou, C., Bruntt, H., Guillot, T., Shporer, A., Guenther, E., Aigrain, S., Almenara, J. M., Alonso, R., Auvergne, M., Baglin, A, *et al.*: 2008 *Astron. & Astrophys.* 488, L47.

Pinheiro da Silva, L. Rolland, Lapeyrere, V. & Auvergne, M.: 2008 *MNRAS* 384, 1337.

Rauer, H., *et al.*: 2008, *Astron. & Astrophys.* , to be submitted.

Weiss, W., Aerts, C., Aigrain, S. *et al.*: 2004, *ESA-SP*, 538, 435